John Mullen is a student at the University of Memphis majoring in Physics with a minor in Mathematics. John will be graduating in the spring of 2025; he hopes to attend graduate school thereafter. In the summer of 2023, John participated in a research experience program funded by the National Science Foundation at the University of Memphis where he worked under Dr. Firouzeh Sabri. John is grateful for the experience the program provided him and hopes to use the skills that he learned to make the world a better place.

John Mullen

Characterization of Collagen Morphology on Aerogel

Faculty Sponsor
Dr. Firouzeh Sabri

Abstract

Type I collagen is the most abundant protein in humans. It is essential to cell attachment and is consequently necessary for cells to thrive. Type I collagen is extensively used in vitro to coat substrates for cell attachment. Aerogel substrates are increasingly being used as medical implants due to their unique physical properties. Therefore, understanding the interaction between collagen and aerogels is important. Despite this, collagen morphology has not been studied extensively on aerogels. This work aims at building a body of knowledge about the dependence of collagen morphology on collagen area-density on two different aerogel substrates. It was observed that collagen fiber length, width, and abundance decreased with increasing collagen area-density on both aerogels tested. Moreover, the collagen film area increased on both substrates with increasing collagen area-density.

Introduction

Aerogels are a class of solid materials that exhibit many unique properties [1], [2]. First and foremost, aerogels are characterized by their highly porous nature, which causes them to be remarkably light for their size [1]. In addition, the physical, chemical, and other properties of aerogels can be easily optimized for specific applications [3]. Moreover, some types of aerogels—including silica-based, polymer, and hybrid aerogels—have been observed to be biocompatible and to have the ability to mimic biological structures [1]. The combination of all these characteristics makes aerogels very attractive materials for biomedical applications. For example, aerogels are currently being used as nerve and cardiovascular implants, among other biomedical applications [3].

Collagen is a class of proteins that are similar chemically, structurally, and functionally [4], [5]. Collagen plays an essential role in cell attachment and providing support for extracellular matrices [4], [5]. Regarding collagen's importance to cell attachment in vivo, cells attach themselves to collagen structures, often in an indirect interaction involving matrix glycoproteins [6]. However, new research suggests that the coevolution of cell adhesion mechanisms and collagens led to the development of cell receptors that bind to specific motifs in collagens [6]. Of the many types of collagens, Type I collagen is the most abundant type in most human tissues [5]. Regarding its role in providing support, type I collagen has the ability to form large fibers which act as structural elements with high tensile strength and low elasticity [4]. Such fibers are extremely common in major connective tissues and are found in select regions of all internal organs [4].

Hence, understanding the interaction between type I collagen and aerogel substrates in vitro is of great interest since cell attachment—to which collagen is essential—is crucial to cell development in vitro. Studying collagen-aerogel interaction could lead to insights about how to improve aerogels for biomedical applications. The work presented here aims at building a body of knowledge of how different area-densities of type I collagen coatings interact with different types of aerogels in vitro. Both collagen fibers and collagen films were investigated, examples of which can be seen in **Figure 1**. The lengths and widths of the collagen fibers, the percentage of the sample's area covered by the collagen film, and the percentage covered by collagen fibers were all measured.

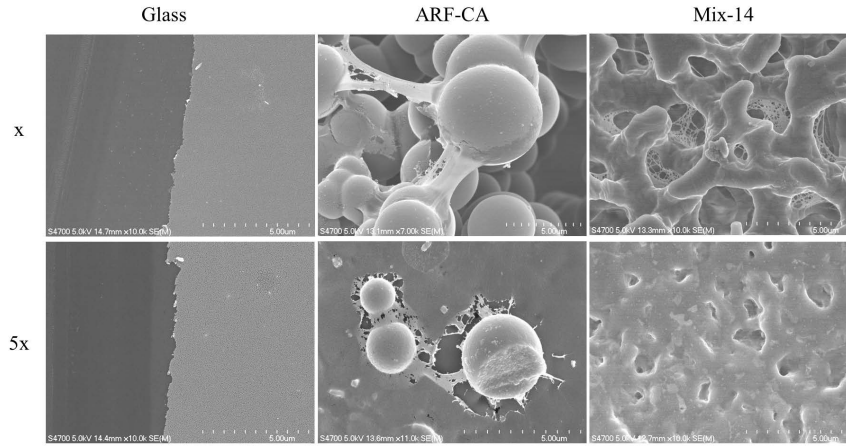

Figure 1 (left to right). Cover glass, ARF-CA, and Mix-14 coated with both 4 $\frac{\mu g}{cm^2}$ (x) and 20 $\frac{\mu g}{cm^2}$ (5x) collagen area-densities. Cover glass is covered with only collagen film; ARF-CA and Mix-14 substrates display both collagen fibers and film.

Materials

Acid-Catalyzed Resorcinol Formaldehyde Carbon Aerogel (ARF-CA)

Carbon aerogels are a subclass of aerogel with extraordinary mechanical, thermal, and electrical properties formed by the organic resorcinol formaldehyde sol-gel process [7]. Resorcinol, formaldehyde, water, and acetic acid were mixed to form the gels from which the samples were made [3]. The gels were cured, soaked in acetone, and super critically dried in liquid CO_2; the resulting aerogels were then heated in a tube furnace under a nitrogen atmosphere at 1050 °C for 3 hours [3].

Superelastic Shape Memory Polyurethane Aerogel (SSMPA) Mix-14

Shape memory aerogels are a new class of aerogel with both the low-density and high-porosity of other aerogels and the characteristics typical of shape-memory materials [3], [8]. Shape memory aerogels have the ability to return to their permanent shape following a temporary deformation. The return to their permanent state is triggered by a stimulus, such as a temperature change. The shape-memory of these aerogels is the result of a triisocyanate core with rigid isocyanurate cross-linking nodes which pull the material back together following deformation [8].

Methods

Collagen Coating

The aerogel samples were cut from a larger piece of material. Great care was taken to ensure that the cutting process did not leave marks on the aerogels, altering their surfaces. In all cases, the face of the aerogel that was in contact with the blade during cutting was the face that the collagen was deposited onto. The aerogel samples were all of similar size and shape, being around 0.5 to 0.7 cm^2, approximately square when viewed from above, and relatively short in height. While the samples were guaranteed to be significantly larger than the size of the collagen structures being studied, the exact dimensions of the samples were not pertinent to the experiment. This step was performed in the same way for the ARF carbon aerogel and the Mix-14. Uncut cover glass from Propper International was used as a control.

The samples were then glued into petri dishes using clear adhesive sealant from Permatex. This was done to ensure that the aerogel samples would be completely submerged by the various baths in the procedure and that they would not simply float on top of the solutions due to their low densities. The glue was allowed to dry for 24 hours before proceeding. The petri dishes were filled with isopropanol (IPA) and allowed to sit for 1 minute. After removing the IPA, the petri dishes were subjected to UV light (λ=254nm) for 20 minutes using a UV chamber, model 234100, from Boekel Scientific.

In an Eppendorf tube, 3 $\frac{mg}{mL}$ rat tail collagen I from Gibco was mixed with 20 mM acetic acid to make enough solution to cover all of the samples with a 20 $\frac{\mu g}{cm^2}$ (5x) area-density coating of collagen, the appropriate volume of solution was placed onto each sample. Great care was taken to ensure that the solution stayed on top of the samples and did not drain into the considerably larger area of the petri dish. The samples were allowed to sit for one hour before proceeding.

The petri dishes were then gently filled with DI water to the point that the samples were submerged. The DI water was removed using a micropipette, and the petri dishes were again filled with DI water. Drops of 2.5% glutaraldehyde with sodium phosphate buffer from Tousimis were added to the petri dishes. After a drop was added, the petri dish was swirled to ensure that the glutaraldehyde was mixed into the solution. In total, 1mL of 2.5% glutaraldehyde was added into the petri dishes. The DI water and glutaraldehyde solution was removed from the dishes using a 1mL micropipette. The dishes were then filled with 2.5% glutaraldehyde to the

point that the samples were submerged. After 2 hours, the glutaraldehyde was removed from the dishes. Two washes were performed with 0.1M sodium phosphate, waiting five minutes between washes. Lastly, six ethanol washes were performed at increasing concentrations (10%, 30%, 50%, 70%, 90%, and 100%) with ten minutes between washes. The ethanol was removed, and the samples were allowed to air dry for 24 hours.

SEM Imaging and Analysis

The samples were sputter coated using a HUMMER 10.2 sputter coater with a gold/palladium target. The current was maintained at 4-5 mA, and the samples were coated for 500 seconds. The samples were imaged using a Phenom scanning electron microscope (SEM). On each sample, a 5-by-5 grid of images was taken at 4800x magnification. The images obtained from the SEM were analyzed with the NIH open-source software ImageJ (version 1.54f). The bar scale put on the images by the SEM was used to calibrate the scale of the measurements in ImageJ. The straight-line tool was used to measure the lengths and widths of the collagen fibers. In addition, the brightness threshold tool was used to determine the percent area of each image covered by the collagen film.

Results

Data is presented for collagen area-densities of both 4 $\frac{\mu g}{cm^2}$ (x) and 20 $\frac{\mu g}{cm^2}$ (5x). Only the data for the 20 $\frac{\mu g}{cm^2}$ area-density is the author's original work.

Collagen Film Area

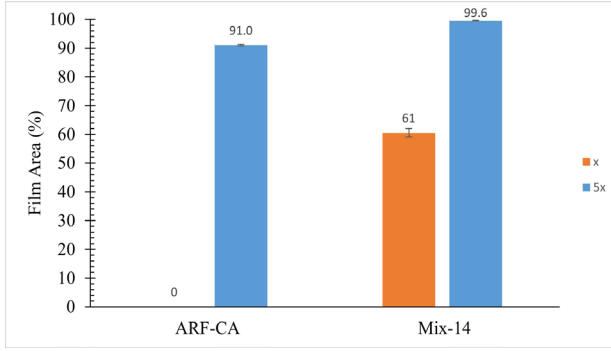

Figure 2. Collagen film area on ARF-CA and Mix-14 at both 4 $\frac{\mu g}{cm^2}$ (x) and 20 $\frac{\mu g}{cm^2}$(5x) collagen area-densities. At "x" collagen area-density, the collagen film covered 0% of the ARF-CA and 61% of the Mix-14 samples, while at "5x" the collagen film covered 91% of the ARF-CA and 99.6% of the Mix-14 samples.

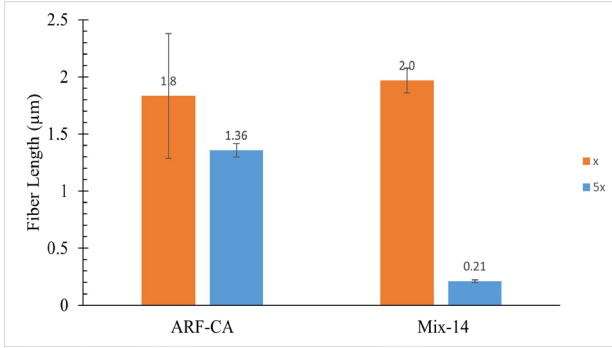

Figure 3. Collagen fiber length on ARF-CA and Mix-14 at both 4 $\frac{\mu g}{cm^2}$ (x) and 20 $\frac{\mu g}{cm^2}$ (5x) collagen area-densities. At "x" collagen area-density, the average collagen fiber length was 1.8µm on ARF-CA and 2.0µm on Mix-14. At "5x" collagen area-density, the average collagen fiber length was 1.36µm on ARF-CA and 0.21µm on Mix-14.

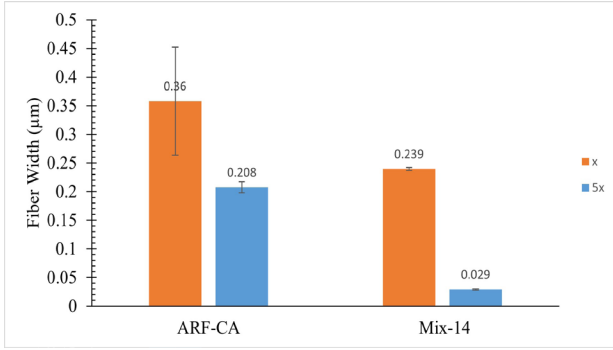

Figure 4. Collagen fiber width on ARF-CA and Mix-14 at both 4 $\frac{\mu g}{cm^2}$ (x) and 20 $\frac{\mu g}{cm^2}$ (5x) collagen area-densities. At "x" collagen area-density, the average collagen fiber width was 0.36µm on ARF-CA and 0.239µm on Mix-14. At "5x" collagen area-density, the average collagen fiber width was 0.208µm on ARF-CA and 0.029µm on Mix-14.

Fiber Area

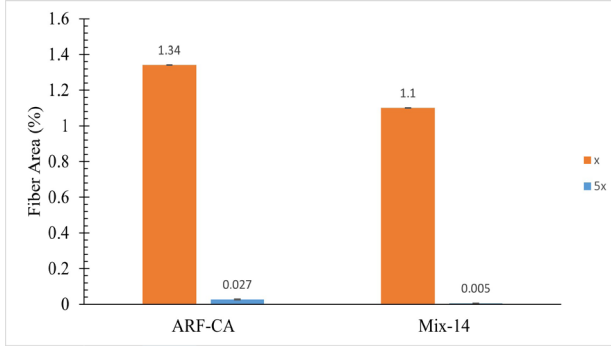

Figure 5. Percentage area of collagen fibers on ARF-CA and Mix-14 at both 4 $\frac{\mu g}{cm^2}$ (x) and 20 $\frac{\mu g}{cm^2}$ (5x) collagen area-densities. At "x" collagen area-density, the collagen fibers covered 1.34% of the ARF-CA and 1.1% of the Mix-14 samples, while at "5x" the collagen fibers covered 0.027% of the ARF-CA and 0.005% of the Mix-14 samples.

Discussion

Collagen Film Area

Figure 2 shows that collagen film area increased on both substrates when collagen area-density increased. The collagen film on Mix-14 was more abundant than that on ARF-CA for both collagen area-densities tested.

Fiber Length and Width

Figure 3 shows a decrease in collagen fiber length with increasing collagen area-density on both ARF-CA and Mix-14. In addition, although the collagen fibers at 4 $\frac{\mu g}{cm^2}$ were of similar lengths on both ARF-CA and Mix-14, the fibers at 20 $\frac{\mu g}{cm^2}$ were significantly shorter on Mix-14 than on ARF-CA. **Figure 4** shows that collagen fiber width decreased with increasing collagen area-density on both ARF-CA and Mix-14. Moreover, the collagen fibers on Mix-14 were narrower than those on ARF-CA regardless of collagen area-density.

Fiber Area

Figure 5 shows that collagen fibers were far more abundant at lower collagen area-densities for both materials. In addition, the fibers on ARF-CA were far more abundant than those on Mix-14 for both collagen area-densities tested.

Conclusion

In conclusion, it was observed that both collagen fiber length and width decreased with increasing collagen area-density on both ARF-CA and Mix-14. In addition, the percentage of the sample area covered by collagen fibers on both ARF-CA and Mix-14 decreased with increasing collagen area-density. Moreover, the collagen film area increased on both substrates with increasing collagen area-density. Lastly, more work is needed to understand why the two aerogels respond differently to an increase in collagen area-density and why collagen tends to form fewer fibers and more film at higher area-densities on both substrates.

References

[1] T. Ferreira-Gonçalves, C. Constantin, M. Neagu, C. P. Reis, F. Sabri, and R. Simón-Vázquez, "Safety and efficacy assessment of aerogels for biomedical applications," *Biomedicine & Pharmacotherapy*, vol. 144, p. 112356, 2021.

[2] M. A. Aegerter, N. Leventis, and M. M. Koebel, *Aerogels handbook*. Springer Science & Business Media, 2011.

[3] M. R. Sala, O. Skalli, and F. Sabri, "Optimal structural and physical properties of aerogels for promoting robust neurite extension in vitro," *Biomaterials Advances*, vol. 135, p. 112682, 2022.

[4] S. Gay and E. J. Miller, "Overview: What is collagen, what is not," *Ultrastruct Pathol*, vol. 4, no. 4, pp. 365–377, 1983.

[5] C. Dong and Y. Lv, "Application of collagen scaffold in tissue engineering: Recent advances and new perspectives," *Polymers (Basel)*, vol. 8, no. 2, p. 42, 2016.

[6] J. Heino, "The collagen family members as cell adhesion proteins," *Bioessays*, vol. 29, no. 10, pp. 1001–1010, 2007.

[7] J. P. Lewicki, C. A. Fox, and M. A. Worsley, "On the synthesis and structure of resorcinol-formaldehyde polymeric networks–precursors to 3D-carbon macroassemblies," *Polymer (Guildf)*, vol. 69, pp. 45–51, 2015.

[8] S. Donthula et al., "Nanostructure-Dependent Marcus-Type Correlation of the Shape Recovery Rate and the Young's Modulus in Shape Memory Polymer Aerogels," *ACS Appl Mater Interfaces*, vol. 10, no. 27, pp. 23321–23334, 2018.